Journal Pre-proofs

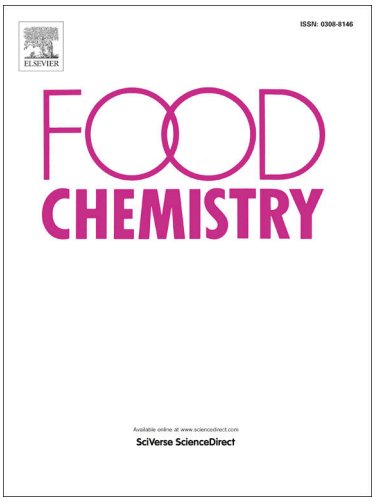


# Simultaneous generation of acrylamide, β-carboline heterocyclic amines and advanced glycation ends products in an aqueous Maillard reaction model system

Wei Quan, Yong Li, Ye Jiao, Chaoyi Xue, Guoping Liu, Zhaojun Wang, Zhiyong He, Fan Qin, Maomao Zeng, Jie Chen

PII: S0308-8146(20)31249-8
DOI: https://doi.org/10.1016/j.foodchem.2020.127387
Reference: FOCH 127387

To appear in: *Food Chemistry*

Received Date: 28 March 2020
Revised Date: 14 June 2020
Accepted Date: 17 June 2020

Please cite this article as: Quan, W., Li, Y., Jiao, Y., Xue, C., Liu, G., Wang, Z., He, Z., Qin, F., Zeng, M., Chen, J., Simultaneous generation of acrylamide, β-carboline heterocyclic amines and advanced glycation ends products in an aqueous Maillard reaction model system, *Food Chemistry* (2020), doi: https://doi.org/10.1016/j.foodchem.2020.127387

# Simultaneous generation of acrylamide, β-carboline heterocyclic amines and advanced glycation ends products in an aqueous Maillard reaction model system

Wei Quan[a], Yong Li[a], Ye Jiao[a, c], Chaoyi Xue[a], Guoping Liu[d], Zhaojun Wang [a], Zhiyong He[a], Fan Qin[a], Maomao Zeng[*, a], Jie Chen[*, a, b]

[a] State Key Laboratory of Food Science and Technology, Jiangnan University, Wuxi, Jiangsu 214122, P R China

[b] Synergetic Innovation Center of Food Safety and Nutrition, Jiangnan University, Wuxi, Jiangsu 214122, P R China

[c] School of Chemistry and Food Engineering, Changsha University of Science & Technology, Changsha 410114, P R China

[d] Wuxi People's Hospital, Nanjing Medical University, Wuxi, Jiangsu 214023, P R China

***Corresponding author:** Prof. Maomao Zeng and Prof. Jie Chen

**E-mail:** mmzeng@jiangnan.edu.cn Chenjie@jiangnan.edu.cn

**Tel.:** +86 510 85919065; Fax: +86 510 85919065

**Abstract**

The simultaneous formation of acrylamide; β-carboline heterocyclic amines (HAs): harmane and norharmane; and advanced glycation end products (AGEs~~):~~ ) (*N*ε-(carboxymethyl)lysine (CML) and *N*ε-(carboxyethyl)lysine (CEL~~);~~ )) was analyzed based on an aqueous model system. The model systems ~~was established to~~ included lysine–glucose (Lys/Glu), asparagine–glucose (Asn/Glu), tryptophan–glucose (Trp/Glu), and a mixture of these amino acids (Mix/Glu). Only AGEs were generated when heated at 100 °C, Asn and Trp competed with Lys for glucose and methylglyoxal (MGO), and glyoxal (GO) decreased AGE content. The *k* value of CML, CEL, and acrylamide decreased when heated at 130 °C, whereas that of harmane increased in the Mix/Glu, owing to the competition between Lys and Asn for glucose, GO, and MGO. Harmane preferably formed *via* the Pictet–Spengler condensation between Trp and acetaldehyde, which further reduced acrylamide formation via the acrolein pathway.

**Keywords:** Multiresponse kinetic models; *N*ε-(carboxymethyl)lysine; *N*ε-(carboxyethyl)lysine; acrylamide; harmane; norharmane

## 1. Introduction

The Maillard reaction (MR) is a non-enzymatic browning reaction due to the complex interaction between free amine groups of amino acids/proteins and carbonyl group of sugars/carbohydrates under the influence of heat (Aljahdali, & Carbonero, 2017; Starowicz, & Zieliński, 2019). MR plays an important role in food processing, because it can form desirable flavors and attractive color compounds in food products (Starowicz, & Zieliński, 2019). However, despite these positive aspects, MR can also form undesirable, potentially toxic, and harmful compounds (Aljahdali, & Carbonero, 2017). One of the Maillard reaction harmful products (MRHPs) that is widely researched is acrylamide, a toxin with mutagenic and carcinogenic properties (Zamani et al., 2017), which was first found and mainly formed in carbohydrate-rich cereals and potato-based foods, such as french fries, potato chips, and baked cookies (Stadler et al., 2002; Zhang, Ren & Zhang, 2009), because asparagine (Asn) is an important precursor for acrylamide (Friedman, 2003; Yaylayan, Wnorowski, & Perez Locas, 2003).

Moreover, advanced glycation end products (AGEs) are a group of structurally complex and chemically stable MRHPs generated at the final MR stage (Poulsen et al., 2013). The most common AGE markers are $N^{\varepsilon}$-(carboxymethyl)lysine (CML) and $N^{\varepsilon}$-(carboxyethyl)lysine (CEL), which have been detected in various kinds of foods, such as cookies, tea, meat products, and potato-based foods (Jiao et al., 2017; Yu et al., 2018). The accumulation of AGEs from the human diet may increase the risk of several chronic diseases in the human body (Poulsen et al., 2013; Singh et al., 2001). Additionally, β-

carboline heterocyclic amines (HAs), including harmane and norharmane, are carcinogenic and neurotoxic MRHPs (Totsuka et al., 1999), which exist in both heat-processed animal- and plant-based foods (Chen et al., 2017; Gibis et al., 2016).

The general reaction scheme of MR and its corresponding MRHPs' formation mechanisms ~~have~~ has been investigated using aqueous model systems of individual amino acids and reducing sugars (Martins, Jongen, & Van Boekel, 2000; Amrein et al., 2006). ~~In detail, t~~The formation of acrylamide ~~has been reportedly~~ follows a generic amino acid route. A Schiff base is formed and then rearranged to yield Amadori products (AP) when a reducing sugar reacts with any amino acid group, followed by decarboxylation and heat-mediated elimination of ammonia to substituted imine, forming acrylamide, with asparagine (Asn) as an important precursor (Yaylayan et al., 2003; Zhang et al., 2009; Zyzak et al., 2003). Several studies revealed that acrylamide can be formed *via* the acrolein pathway, and acrolein was reportedly generated through ~~ethanal~~acetaldehyde oxidation (Becalski et al., 2003; Zyzak et al., 2003). Similar to acrylamide, CML and CEL can be formed through AP formation directly or through a reaction between lysine (Lys) and reactive α-dicarbonyl compounds, including methylglyoxal (MGO) and glyoxal (GO), which are generated in the middle MR stage (Singh et al., 2001; Srey et al., 2010). Moreover, β-carboline HAs (harmane and norharmane) formation is partly different from that of acrylamide and AGEs. Herraiz (2000) indicated that tetrahydro-β-carboline (THβC) oxidation is another way to produce β-carboline HAs, and that the Pictet–Spengler condensation between Trp and acetaldehyde is the most effective way to form THβCs, except for AP dehydration and

β-elimination (Gibis et al., 2016).

The precursors, including Lys, Asn, and Trp, always exist together in some real food systems, especially ~~for~~ cereals and potato-based foods (Choi et al., 2016). Several studies have indicated that adding Lys and Trp was effective in inhibiting the formation of acrylamide in an aqueous MR model system, but AGE and β-carboline HA formation was not considered (Kim, Hwang, & Lee., 2005; Koutsidis et al., 2009). Furthermore, in several cereals and potato-based foods, the concentration of reducing sugars is relatively lower than that of the free amino acids, and the content of each amino acid is different (Choi et al., 2016). Thus, with such limited amounts of reducing sugars, Lys, Asn, and Trp competed with each another to participate in the MR, which could show different kinetic results MRHP formation, compared with that of model systems of individual amino acids and reducing sugars. However, less attention has been given to the simultaneous acrylamide, AGE, and β-carboline HA generation ~~in~~ under such conditions.

Therefore, we aimed to investigate simultaneous acrylamide, β-carboline HA (harmane and norharmane), and AGE (CML and CEL) formation based on an aqueous model system with a limited content of reducing sugars and different concentrations of precursor amino acids, using multi-response kinetic modeling. Compared with single-response modeling, multi-response modeling can be more rigorously tested, and the estimation of model parameters can be accurately performed (Martins et al., 2000; Nguyen & Van Boekel, 2017). The present study ~~would~~ gives an insight into the effects of precursor amino acids on simultaneous acrylamide, β-carboline HA (harmane and

102 norharmane), and AGE (CML and CEL) formation, which were found to be generated
103 in cereals and potato-based foods.

104 ## 2. Materials and methods

105 ### 2.1 Chemicals

106 Chemical standards of glucose and $^{13}C_6$-glucose, amino acids (Lys, $d_4$-Lys, Trp, and
107 Asn), intermediates (acetaldehyde, acrolein, glyoxal, and methylglyoxal), HAs
108 (harmane and norharmane), and nonafluoropentanoic acid (NFPA, purity over 97%)
109 were purchased from J&K Scientific Co., Ltd. (Beijing, China). The standards of CML,
110 $d_4$-CML, CEL, and $d_4$-CEL were provided by Santa Cruz Biotechnology Co. (Paso
111 Robles, CA). ~~acrylamide~~ Acrylamide and $^{13}C_3$-acrylamide were purchased from Sigma-
112 Aldrich. High-performance liquid chromatography (HPLC~~) )~~-grade methanol and
113 acetonitrile were obtained from Tedia Company Incorporated (Fairfield, OH~~, USA~~).
114 The other chemicals were all analytical grade and were purchased from Sinopharm
115 Chemical Reagent Co., Ltd. (Shanghai, China).

116 ### 2.2 Model systems and reaction conditions

117 The aqueous model system was established as previously described (Nguyen et al.,
118 2016; Yu et al., 2020), with slight modifications. Four amino acid–glucose reaction
119 solutions containing Lys–glucose (Lys/Glu; 30 mmol/100 mmol), Asn–glucose
120 (Asn/Glu; 200 mmol/100 mmol), Trp–glucose (Trp/Glu; 5 mmol/100 mmol), or a
121 combination of Lys–Asn–Trp–glucose (Mix/Glu; 100 mmol/200 mmol/5 mmol/100
122 mmol) were prepared in phosphate buffer (0.1 M, pH 7.0). The Lys, Asn, Trp, and
123 glucose concentrations selected in the model system were based on their actual

proportions in real cereal and potato-based foods (Choi et al., 2016; Halford et al., 2012), and their concentrations were appropriately magnified to better evaluate the intermediates and final products. The 10-mL reaction samples were added to glass reaction vials with Teflon caps (Synthware, Beijing, China) to avoid side phenomena, such as water evaporation or oil absorption. The samples were pre-heated at 100 °C and 130 °C, respectively, in a thermostat-controlled oil bath with a magnetic stirrer (Jintan, Zhejiang, China) for 5 min. The purpose of pre-heating is to raise the temperature of the samples to the intended temperature level. The temperature of the oil bath was checked every 1 min, and the temperature fluctuations were within 3 °C. The reaction time was recorded after the pre-heated treatment. Samples were taken at each predetermined heating time (3, 6, 9, 12, 15, 18, and 21 min), the vials were immediately cooled in an ice bath to stop any further reaction, and then they were stored at −20 °C prior to analysis. The model system experiments were performed in triplicate.

**2.3 Analysis of melanoidins**

Melanoidins were measured by using an UV-Vis spectrophotometer (UV-1601~~,~~; Shimadzu, Kyoto, Japan) with a path length of 1 cm at 470 nm, and then the samples were diluted. The results were calculated using the Lambert~~—~~Beer equation with an extinction coefficient of 282 L $mol^{-1}cm^{-1}$, as reported by Zhang et al. (2015), with the following equation:

$$A = \varepsilon \times bc$$

where, A is the absorbance value at 470 nm, ε is an extinction coefficient, b is the thickness of the container's absorbent layer, and c is the melanoid molar concentration.

## 2.4 Analysis of CML and CEL

CML and CEL sample analysis were performed according to the methods previously described by Jiao et al (2017), and Yu et al (2018). Each 150-μL reaction sample was mixed with 150 μL $d_4$-CML and $d_4$-CEL (internal standards), followed by centrifugation at 10,000 rpm for 10 min and filtration through a 0.22-μm membrane. The obtained filtrate was separated using Waters 2695 liquid chromatography (LC) module with a Waters X-Bridge C18 column at 35 °C (2.1 mm × 100 mm; 3.5 μm; Milford, MA~~, USA~~). The mobile phase consisted of acetonitrile as solvent **A** and 5 mM NFPA as solvent **B**, and gradient elution with a flow rate of 0.3 mL/min was performed as follows: 0–5 min, 5%–60% **A**; 5–7 min, 60%–100% **A**; 7–9 min, 100% **A**; 9–10 min, 100%–5% **A**; and 10–16 min, 5% **A**. Injection volume was set to 5 μL, and detection was performed using a Micromass Quattro micro triple quadrupole mass spectrometer (Manchester, UK) using the electrospray ionization positive mode with the multiple reaction monitoring (MRM) model. The capillary voltage was 3.5 kV, and the ionization source and desolvation gas temperatures were 110 °C and 400 °C, respectively. The nitrogen flow rates were 50 and 600 L/h for the cone gas and desolvation gas, respectively, whereas the cone and collision energies were 20 V and 18 V, respectively. For CML, $d_4$-CML, CEL, and $d_4$-CEL, the fragments *m/z* 205→84, *m/z* 209→88, *m/z* 219→84, and *m/z* 223→88 were used for quantification, respectively. CML and CEL quantification was done using isotope internal standard method.

## 2.5 Analysis of GO and MGO

The α-dicarbonyl compound derivatization was performed with 100 μL of 5 μM *o*-

phenylenediamine, as previously described (Scheijen & Schalkwijk, 2014). Reaction samples were centrifuged at 10,000 ×*g* for 10 min, and the 200-µL supernatant was derivatized, then 100 µL 2,3-hexanedione (4 µM) was added as the internal standard and immediately mixed and kept at 4 °C in the dark for 12 h prior to HPLC–MS/MS measurement.

According to Jiao et al (2019) the quinoxaline derivatives of the α-dicarbonyl compounds were determined using Waters 2695 LC system interfaced with a Micromass Quattro micro triple quadrupole mass spectrometer. Separation was performed on a Waters X-Bridge C18 column (2.1 mm × 100 mm; 3.5 µm) using a gradient mixture of (**A**) 1% formic acid in water and (**B**) methanol at 0.3- mL/min flow rate. The elution gradient was as follows: 0–5 min, 30%–90% **A**; 5–8 min, 90%–100% **A**; 8–10 min, 100% **A**; 10–12 min, 100%–30% **A**; and 12–15 min, 30% **A**. The α-dicarbonyl compound identification was performed using the MRM mode with the same MS parameters as those used in CML and CEL detection. The fragments *m/z* of the quinoxaline derivatives of α-dicarbonyl compounds were *m/z* 131→77 (GO), 145→77 (MGO), and 187→77 (internal standard).

### 2.6 Simultaneous determination of acrylamide, harmane, norharmane, amino acids, and glucose using UHPLC-MS/MS

The reaction sample (150 µL) was added to the 150- µL internal standard solution containing 200 µg/mL $^{13}C_3$-acrylamide, 500 µg/mL $d_4$-Lys, and 500 µg/mL $^{13}C_6$-glucose, centrifugated at 10,000 rpm for 10 min, and filtered through a 0.22-µm membrane. The obtained filtrate was collected for UHPLC–MS analysis as previously

described by Zhang et al (2011), with slight modifications.

The identification and quantification were conducted using an ACQUITY UHPLC system equipped with a triple quadrupole mass spectrometer (Waters, Milford, MA, ~~USA~~). Analyte separation was performed on a Waters Atlanti~~c~~s dC18 column (250 mm × 4.6 mm i.d.; 3.0 μm particle size) at 30 °C. The gradient elution was obtained with a binary mobile phase of 0.1% formic acid (pH 6.8; solvent **A**) and acetonitrile (solvent **B**). The solvent composition was 0–0.1 min, 5% **A**; 0.1–10 min, 5%–100% **A**; 10–10.5 min, 100%−5% **A**; and 10.5–15 min, 5% **A**. The flow rate was set to 0.5 mL/min, with a 5-μL injection volume. Mass spectrometric detection was performed in the MRM mode. The capillary voltage was 3.5 kV, and the ion source and desolvation gas temperatures were 130 °C and 350 °C, respectively. The fragments used for quantification were *m/z* 133→74 (Asn), 147→84 (Lys), 151→88 ($d_4$-Lys), 205→188 (Trp), 72→55 (acrylamide), 75→58 ($^{13}C_3$-acrylamide), 151→88 ($d_4$-Lys), 169→115 (norharmane), 183→115 (harmane), 383→203 (glucose), and 395→209 ($^{13}C_6$-glucose).

**2.7 HPLC analysis of acrolein**

By using a previously reported model with slight modifications (Barman, 2014; Uchiyama, Inaba & Kunugita, 2011), a 2.5-mL reaction sample was placed in a 10-mL centrifugation tube. Afterward, 1 mL 2% NaCl–0.7 mol/L HCl solution, 0.5 mL 18% $Na_2HPO_4$, and 0.5 mL 0.2% 2,4-dinitrophenylhydrazine solution were sequentially added. Water was added to a volume of 10 mL, and the contents were mixed through shaking before heating in a water bath at 60 °C for 20 min. Upon cooling to room temperature, 3 mL of hexane ~~was~~ were twice added for acrolein extraction, and 1 mL

of hexane was filtered through a 0.22-μm organic microporous membrane and subjected to HPLC analysis.

A LiChrospher® C18 (4.6 mm × 250 mm~~;~~ , 5.0 μm) column was used to separate 2,4-dinitrophenylhydrazones. The injection volume was set to 10 μL, and the column temperature was maintained at 30 °C. The solvent flow rate was 1.0 mL/min under an isocratic water–acetonitrile elution (38:62; v/v) for 20 min. The acrolein derivatives (2,4-dinitrophenylhydrazones) were detected using a UV detector at 365 nm.

**2.8 Headspace gas chromatography analysis of acetaldehyde**

According to Qin et al (2020), acetaldehyde analysis was performed with an HS-10 automated headspace sampler (Shimadzu, Kyoto, Japan) and GC-2010 gas chromatograph~~y~~ (Shimadzu, Kyoto, Japan), with a flame ionization detector and a DB-23 capillary column (~~i.d.~~ 60 m × 0.32 mm i.d., ~~×~~ 0.25 μm film thickness~~; 60 m) (;~~ Agilent Technologies, ~~California, USA~~Folsom, CA). The 3 mL reaction solution aliquot was added to a 20-mL vial, sealed, and then heated at 75 °C for 30 min on the headspace sampler. The transfer line temperature was 120 °C. The gas flow was set to 2.0 mL/min, and the detector and injection temperatures were 260 °C and 205 °C, respectively. The column was maintained at 35 °C for 6 min and was heated to 185 °C at an incremental rate of 10 °C/min. Furthermore, the analysis was set to 1:1 split mode.

**2.9 Method validation**

The proposed method's linearity, recovery, limit of detection, and limit of quantification were evaluated. Calibration curve was established by plotting the peak area ratios or only the peak area of the standards to the internal standard against the

eight analyte concentrations. Sample preparation recoveries were determined by analyzing blank samples spiked with two concentrations of mixed low and high standards, and they were calculated as [(levels in spiked samples − levels in blank samples)/amount added] × 100. The overall method's precision was determined by implementing intra-day (repeatability) and inter-day (reproducibility) precision experiments. Intra-day precision was evaluated at a low spiked level through a recovery study with three replicates, whereas inter-day precision was evaluated at a high spiked level through a recovery study that was consecutively carried out for 3 days.

**2.10 Multi-response kinetic modeling**

A comprehensive reaction mechanism was built, comprising the major formation pathways of the MR and caramelization (see Fig. 5). The average duplicate analysis data results were normalized and expressed in millimoles per liter (mmol/L). All experiment data were made to fit the proposed kinetic model, and the kinetic parameters (*k)* were estimated using the non-linear curve fitting function of the Origin 9.0 software (OriginLab, Northampton, MA~~USA~~) and SAS 8.0 software (SAS Institute Inc., China), and ~~the R-squared (~~$R^2$~~)~~ values were calculated to determine the fitting performance of the non-linear fitted models (Yu et al., 2020; Zhang et al., 2015). Furthermore, the experiments were performed at only one or two temperatures; hence, specific activation energies cannot be estimated.

~~**2.11 Statistical analysis**~~

~~The component analysis was conducted in triplicate, with values reported as the mean ± standard deviation of three independent experiments. Statistical analysis was~~

~~performed using the general linear model protocol of Statistix 9.0 software (Analytical Software, Tallahassee, FL, USA). Analysis of variance of the results and subsequent least significant difference post hoc test were performed to determine significant differences ($p < 0.05$) among different MR model systems.~~

### 2.11 Statistical analysis

The analysis of all components was conducted in triplicate, with values reported as the mean ± standard deviation (SD) of three independent experiments. Statistical analysis was performed using the general linear model procedure of Statistix software 9.0 (Analytical Software, Tallahassee, FL~~, USA~~). Analysis of variance of the results followed by the least significant difference post hoc test was performed to determine ~~whether~~ if there were significant differences ($p < 0.05$) among different MR model system.

## 3. Results and discussion

### 3.1 Reactant concentration during heating

Figure 1 shows the amino acid and glucose kinetic profiles during heating. As expected, amino acid and glucose concentrations decreased with increased heating time, which was consistent with a previous report (Zyzak et al., 2003). As shown in Figure 1A, the final Trp, Lys, and Asn concentrations in the Trp/Glu, Lys/Glu, and Asn/Glu models decreased by 20.7%, 29.1%, and 33.3%, respectively, when heated at 100 °C, compared with their initial concentrations; however, ~~that~~ concentrations in the Mix/Glu model were reduced by 6.0%, 19.3%, and 30.9%, respectively, compared with their

initial concentrations. Trp, Lys, and Asn concentrations in the Trp/Glu, Lys/Glu, and Asn/Glu decreased by 79.2%, 56.1%, and 52.0%, respectively, when the heating temperature changed to 130 °C (Fig. 1B). However, Trp, Lys, and Asn concentrations in the Mix/Glu model were only reduced by 10.9%, 38.7%, and 50.1%, respectively. The results suggest that Trp and Lys degradation in the Mix/Glu model was significantly less than that for the Trp/Glu and Lys/Glu models. However, Asn consumption in the Asn/Glu and Mix/Glu models showed insignificant differences.

Glucose concentration was monitored during heating (Figs. 1C and 1D). Glucose consumption levels in the Asn/Glu, Mix/Glu, Lys/Glu, and Trp/Glu models were only 24.1%, 28.1%, 15.7%, and 15.8% of their initial concentrations, respectively, when heated at 100 °C. However, the glucose consumption in each of the Trp/Glu, Asn/Glu, Mix/Glu, and Lys/Glu models increased by 66.1%, 73.2%, 95.5%, and 63.1%, respectively, when heated at 130 °C. Glucose reduction levels in the Trp/Glu and Lys/Glu models were significantly less than ~~that~~ those for the Asn/Glu and Mix/Glu models.

### 3.2 Formation of acrylamide and HAs during heating

The formation of acrylamide was measured and shown in Figure 2A. There was no acrylamide produced at 100 °C due to the low reaction temperature. This finding is consistent with previous literature (Zhang et al., 2009). When heated at 130 °C, acrylamide was generated after 6 min at 130 °C. The content of acrylamide in the Asn/Glu and Mix/Glu models reached a maximum of 22.9 ± 2.55 μg/mL and 12.6 ± 2.80 μg/mL, respectively. In comparison, the production of acrylamide was

significantly reduced by 45.2% ($p < 0.05$) when Trp and Lys were involved in the reaction. This is consistent with previous studies by Koutsidis (2009) and Mestdagh et al (2008), who reported that Trp and Lys may reduce the concentration of acrylamide.

Two HAs, harmane and norharmane, were undetectable when the model mixtures were heated at 100 °C (Fig. 2A). Several published studies have reported that HAs were generated at temperatures generally higher than 125 °C (Gibis, 2016). When the models were heated at 130 °C, norharmane could be detected after 6 min, and its highest concentrations reached in the Trp/Glu and Mix/Glu models were 27.9 ± 2.03 ng/mL and 22.6 ± 1.74 ng/mL, respectively. Norharmane content in the Trp/Glu model was significantly higher ($p < 0.05$) than that in the Mix/Glu model; however, harmane was detected only after 15 min of heating time in the Trp/Glu and Mix/Glu models (Fig. 2B). Harmane content in the Trp/Glu model ranged from 13.5 ± 0.90 to 13.9 ± 0.68 ng/mL and was significantly increased ($p < 0.05$) by 6.6~~%~~–13.1% in the Mix/Glu model, which was exactly in contrast to the norharmane results.

### 3.3 Formation of AGEs and melanoidins in the model systems

As shown in Figure 2D and 2E, CML and CEL were generated at both 100 °C and 130 °C~~, respectively~~. CML contents in the Mix/Glu and Lys/Glu models were 5.11 ± 1.03 μg/mL and 11.6 ± 2.21 μg/mL, respectively, when heated at 100 °C, whereas th~~at~~ose of CML in the same models were 9.06 ± 1.89 μg/mL and 27.2 ± 2.31 μg/mL, respectively, when heated at 130 °C. Furthermore, CEL content was 8.30 ± 3.15 μg/mL for the Mix/Glu model and 10.6 ± 0.49 μg/mL for the Lys/Glu model when heated at 100 °C. Moreover, it significantly increased to 31.9 ± 8.09 μg/mL and 51.7 ± 8.74

322 μg/mL for the Mix/Glu and Lys/Glu models, respectively, when heated at 130 °C. These
323 results show that CML and CEL contents generated at 130 °C were higher than their
324 contents at 100 °C. CML formation in the Mix/Glu model was significantly lower ($p <$
325 0.05) than that for the Lys/Glu model.

326 Melanoidins, generated by aldol condensation and carbonyl compound
327 polymerization, ~~were~~ are considered the main products in the final MR stage (Martins
328 et al., 2000; Wang, Qian & Yao, 2011). Generally, melanoidin generation in all groups
329 exhibited a minimal increase during heating (Fig. 2F and 2G), and melanoidin content
330 reached a maximum at the end of the reaction. The highest melanoid concentrations
331 ~~was~~ were observed in the Mix/Glu model (at 3.37 ± 0.94 mmol/L and 30.8 ± 0.75
332 mmol/L) when melanoidins were heated at 100 °C and 130 °C, whereas the lowest
333 concentrations ~~was~~ were found in the Trp/Glu model.

334 **3.4 Formation of α-dicarbonyl compounds**

335 The α-dicarbonyl compounds, including GO and MGO, are highly reactive
336 intermediates that play an important role in MR (Martins et al., 2000). They are mainly
337 produced by thermal glucose degradation and Schiff base decarboxylation, which reacts
338 with amino acids to form a series of MRHPs (Chen & Kitts, 2011). Figure 3 shows the
339 GO and MGO amounts that were detected. A higher GO concentration can be found at
340 130 °C than at 100 °C. The GO concentration in different model systems increases with
341 reaction time, except for the Trp/Glu and Lys/Glu models, which showed a maximum
342 GO concentration at the initial stage, but significantly decreased when heated at 100 °C
343 and 130 °C, respectively. A comparison of the different model systems showed that the

Lys/Glu model has the highest GO contents when heated at both 100 °C and 130 °C, with a range of 3.01 ± 0.50 to 7.38 ± 1.54 μg/mL and 8.33 ± 1.81 to 35.1 ± 0.43 μg/mL, respectively, followed by the Mix/Glu model.

A significant increase in MGO concentration was observed with increased reaction time, reaching a relatively high value at the end of the reaction (Figs. 3B and 3D). Similar to GO, higher temperatures induced easier MGO formation ~~of MGO~~. MGO generation in the different model systems varied ~~relatively.~~ . The MGO levels produced in the Mix/Glu and Lys/Glu models were higher than ~~that~~ those in other systems ~~when~~ heated at 100 °C. However, the Mix/Glu and Asn/Glu models showed the highest MGO content when heated at 130 °C.

### 3.5 Formation of aldehyde compounds

Aldehydes are also important MR intermediates and are known as glucose degradation products at high temperatures (Martins et al., 2000; Van Boekel, 2006). Lys/Glu had higher reactivity levels and generated more ~~ethanal~~acetaldehyde than the other models at the two heating temperatures (Figs. 4C and 4D). The ~~ethanal~~acetaldehyde contents in the Lys/Glu model system ~~was~~ were 3.02 ± 0.12 μg/mL at 100 °C and 13.1 ± 1.13 μg/mL at 130 °C. Moreover, Asn/Glu also produced a higher ~~ethanal~~acetaldehyde content of 12.2 ± 1.53 μg/mL when heated at a higher temperature.

Acrolein is an important intermediate compound that can form acrylamide via the acrolein pathway, which is mainly produced by ~~ethanal~~acetaldehyde oxidation (Becalski et al., 2003; Zyzak et al., 2003). The acrolein content showed ~~an~~ ia non-significant difference among the model systems when heated at 100 °C (Fig. 4A).

However, the highest acrolein concentration was observed in the Lys/Glu and Trp/Glu models, which ranged from 0.06 ± 0.01 to 1.29 ± 0.12 μg/mL and from 0.20 ± 0.09 to 1.25 ± 0.09 μg/mL, respectively, when heated at 130 °C (Fig. 4B).

### 3.6 Validation of the proposed analytical methods

The characteristics of the proposed method were demonstrated by a validation procedure of the linearity, LOD, LOQ, recovery, and precision of the method. The linearity was evaluated by injecting different concentrations of standards and plotting the peak areas *versus* the concentrations (Yan et al., 2014). As shown in Supplemental Tables 1 and 2, the detector response for individual compounds was linear over a broad concentration range, with coefficients higher than 0.991. The LODs and LOQs, which are respectively defined as the amount of an analyte producing a signal-to-noise ratio of ≥3 and ≥10, were determined using standards. The recoveries of compounds in the model system ranged from 87.1% to 116% at a low spiked level and from 83.1% to 123% at a high spiked level. The precisions, which are expressed as relative standard deviations (RSDs) were lower than 15.3% (14.6%) for intraday (interday) studies. By summarizing all of these method validation results, the developed method proposed here can be regarded a potent quantification method that could be successfully applied to the analysis of reactants, products, and intermediate compounds in a Maillard reaction model system corresponding to the kinetic study, with appropriate recoveries and excellent method repeatability.

### 3.7 Reaction kinetic modeling and related parameters

Referring to the general mechanisms of MRHPs reported in previous literature (Gibis

388 et al., 2016; Srey et al., 2010; Yaylayan et al., 2003; Zyzak et al., 2003), the reaction
389 scheme was simplified into an apparent scheme (Fig. 5) by keeping only the reactants
390 (Lys, Trp, Asn, and glucose), aldehydes, and ketone intermediates (acrolein,
391 acetaldehyde, GO, and MGO), and final products (CML, CEL, harmane, norharmane,
392 acrylamide, and melanoidins). Due to the different reaction rate constants, several
393 intermediates showed higher uncertainty and, thus, could not be estimated in this
394 interval, such as AP which could not be quantified analytically. Kinetic data were fitted,
395 and the related kinetic parameters ($k_1$–$k_{11}$) were calculated by the non-linear least
396 squares regression, according to previous studies (Yu et al., 2020; Zhang et al., 2015).
397 $R^2$ values were calculated to evaluate the model-fitting performance. As shown in Table
398 1, most models showed high $R^2$ values, ranging from 0.80–0.99, which reflected good
399 fitting to the proposed reaction scheme.

400 Table 1 shows the $k$ values for the formation and elimination of the reactants,
401 intermediates, and MRHPs. The $k$ values generally increased with temperature in all
402 the model systems, which may be due to the enhanced molecular mobility at high
403 temperatures, and this was consistent with the general rule of kinetics (Martins et al.,
404 2000). Mel formation in all models showed the highest $k$ value. Furthermore, owing to
405 the lower heating temperature (100 °C), acrylamide, harmane, and norharmane were
406 not detected; hence, the values of $k_5$, $k_8$, $k_9$, and $k_{10}$ were considered zero.
407 Simultaneously, comparing the rate constants of the different model systems at 100 °C
408 revealed that another $k$ value in the Lys/Glu model was significantly higher than that
409 for the other model systems, although the $k$11 value of the Lys/Glu model is lower than

that of the Mix/Glu model. The results indicated that the MR in the aqueous model system mainly involved a reaction with Lys and glucose to form CML and CEL when heated at 100 °C, which may be due to the high activity of Lys in the MR, depend~~ing~~ent on the number of carbon (C) atoms and its epsilon amino group in the amino acid molecule (Claeys et al., 2005; De Sa et al., 2010). Moreover, compared with the Lys/Glu model, the lower *k* values for GO, MGO, CML, and CEL ($k_1$, $k_2$, $k_3$, and $k_4$) in the Mix/Glu model indicated that the decreased CML and CEL concentrations in the Mix/Glu may be attributed to Asn and Trp competing with Lys for the GO and MGO in the MR when heated at 100 °C.

The comparison of kinetic parameters between the Lys/Glu, Asn/Glu, and Mix/Glu models when heated at 130 °C revealed that the *k* values for CML, CEL, and acrylamide ($k_3$, $k_4$, and $k_5$) and those for α-dicarbonyl compounds ($k_1$ and $k_2$) in the Mix/Glu model system were significantly lower ($p < 0.05$) than ~~that~~ those in the Lys/Glu and Asn/Glu model systems. Previous studies found that adding Lys to the Asn/Glu model can significantly reduce the acrylamide production due to the high Lys activity in the MR from competing with Asn for the reducing sugar (Koutsidis et al., 2009; Mestdagh et al., 2008). However, those studies have not considered CML and CEL formation, except for the competitive inhibition between Lys and Asn on acrylamide formation. Several studies have reported that Lys could decrease acrylamide formation *via* adduct formation (Claeys et al., 2005; Friedman et al., 2003). These adducts are due to the electrophilic double bond of acrylamide, which can participate in nucleophilic reactions with active hydrogen-bearing functional groups, such as the $–NH_2$ group of Lys.

Furthermore, the adduct reaction between Lys and acrylamide not only decreased acrylamide formation but may also reduce CML and CEL generation by Lys consumption. Furthermore, the significantly decreased CML, CEL, and acrylamide formation may be due to their competition for α-dicarbonyl compounds between Asn and Lys (particularly GO) (Amrein et al., 2006).

The $k$ values for norharmane ($k_{10}$) and acrylamide ($k_8$) in the Mix/Glu model were significantly reduced, compared with the Trp/Glu and Asn/Glu models. Previous studies reported that Trp may compete with Asn for reducing sugars, and a non-covalent interaction occurred between acrylamide and Trp (Koutsidis et al., 2009). Therefore, adding Trp to the Asn/Glu model can significantly reduce acrylamide production (Koutsidis et al., 2009). However, a significant increase in harmane content ~~that was generated~~ in the Mix/Glu model was observed. Table 1 shows that acetaldehyde formation ($k_6$) in the Mix/Glu model was significantly increased, compared with the Trp/Glu model, which contributed to harmane formation, because acetaldehyde is an important intermediate for β-carboline HA formation. The details of this reaction show that acetaldehyde can be used to form THβC through Pictet–Spengler condensation, and can further generate harmane through THβC oxidation (Herraiz, 2000). The $k$ values of acetaldehyde and acrolein in the Mix/Glu model were significantly decreased, compared with the Asn/Glu model, and the resulting $k$ value of acrylamide ($k_8$) produced by the acrolein oxidation pathway was significantly reduced. Therefore, we speculated that the competition for acetaldehyde between Asn and Trp and further inhibition of acrolein formation may be the reason for the increased harmane content

and decreased acrylamide content in the Mix/Glu model when heated at 130 °C.

## 4. Conclusions

In this study, aqueous MR model systems, including Asn/Glu, Lys/Glu, Trp/Glu, and Mix/Glu, were established to investigate simultaneous acrylamide, CML, CEL, harmane, and norharmane formation. The results indicated that only CML and CEL were generated when heated at 100 °C, and they would compete with Lys for GO and MGO in the presence of Asn and Trp, thus leading to significantly decreased CML and CEL concentrations. ~~acrylamide~~Acrylamide, CML, and CEL were similarly reduced when heated at 130 °C because of the competition between Asn and Lys for glucose and α-dicarbonyl compounds. However, harmane levels were increased through Pictet–Spengler condensation when Trp reacted with acetaldehyde in the Mix/Glu system. Moreover, it would further reduce acrolein formation by consuming acetaldehyde, thus inhibiting acrylamide formation *via* the acrolein oxidation pathway. Therefore, this study revealed the effects of Asn, Lys, and Trp on simultaneous AGEs, β-carboline HAs, and acrylamide generation. Further studies are warranted to examine the obtained insights regarding the complex interactions and key factors that affect MRHP generation in real food systems, which in turn will influence the identification of mitigation strategies during food processing.

## Acknowledgements

The National Key R & D Program of China (Grant No.2017YFC1600405, Grant No.

2018YFC1600405). The Key Research and Development Plan of Guangdong Province, China (Grant No.2019B020212011). The National First-class Discipline Program of Food Science and Technology (No. JUFSTR20180201).

## References

Aljahdali, N., & Carbonero, F. (2017). Impact of Maillard reaction products on nutrition and health: Current knowledge and need to understand their fate in the human digestive system. *Critical Review in Food Science and Nutrition*, 1-14.

Amrein, T. M., Andres, L., Manzardo, G. G., & Amadò, R. (2006). Investigations on the promoting effect of ammonium hydrogencarbonate on the formation of acrylamide in model systems. *Journal of Agricultural and Food Chemistry*, *54*(26), 10253-10261.

Barman, B. N. (2014). Accurate determination of aldehydes in amine catalysts or amines by 2, 4-dinitrophenylhydrazine derivatization. *Journal of Chromatography A*, *1327*, 19-26.

Becalski, A., Lau, B. P. Y., Lewis, D., & Seaman, S. W. (2003). Acrylamide in foods: Occurrence, sources, and modeling. *Journal of Agricultural and Food Chemistry*, *51*(3), 802-808.

Chen, X. M., & Kitts, D. D. (2011). Identification and quantification of α-dicarbonyl compounds produced in different sugar-amino acid Maillard reaction model systems. *Food Research International*, *44*(9), 2775-2782.

Choi, S. H., Kozukue, N., Kim, H. J., & Friedman, M. (2016). Analysis of protein amino acids, non-protein amino acids and metabolites, dietary protein, glucose, fructose, sucrose, phenolic, and flavonoid content and antioxidative properties of potato tubers, peels, and cortexes (pulps). *Journal of Food Composition and Analysis*, *50*, 77-87.

Claeys, W. L., De Vleeschouwer, K., & Hendrickx, M. E. (2005). Effect of amino acids on acrylamide formation and elimination kinetics. *Biotechnology Progress*, 2*1*(5), 1525-1530.

De Sa, P. F., Treubig Jr, J. M., Brown, P. R., & Dain, J. A. (2001). The use of capillary electrophoresis to monitor Maillard reaction products (MRP) by glyceraldehyde and the epsilon amino group of lysine. *Food Chemistry*, *72*(3), 379-384.

Friedman, M. (2003). Chemistry, biochemistry and safety of acrylamide. A review. *Journal of Agricultural and Food Chemistry*, *51*, 4504−4526.

Gibis, M. (2016). Heterocyclic aromatic amines in cooked meat products: causes, formation, occurrence, and risk assessment. *Comprehensive Reviews in. Food Science and Food Safety*, *15*(2), 269-302.

Halford, N. G., Muttucumaru, N., Powers, S. J., Gillatt, P. N., Hartley, L., Elmore, J. S., & Mottram, D. S. (2012). Concentrations of free amino acids and sugars in nine potato varieties: effects of storage and relationship with acrylamide formation. *Journal of Agricultural and Food Chemistry*, *60*(48), 12044-12055.

Herraiz, T. (2000). Analysis of the bioactive alkaloids tetrahydro-β-carboline and β-carboline in food. *Journal of Chromatography A*, *881*(1-2), 483-499.

Jiao, Y., He, J., Li, F., Tao, G., Zhang, S., Zhang, S., Fan, Q., Zeng, M., & Chen, J. (2017). Nε-(carboxymethyl) lysine and Nε-(carboxyethyl) lysine in tea and the factors affecting their formation. *Food Chemistry*, *232*, 683-688.

Jiao, Y., Quan, W., He, Z., Gao, D., Qin, F., Zeng, M., & Chen, J. (2019). Effects of Catechins on N ε-(Carboxymethyl) lysine and N ε-(Carboxyethyl) lysine Formation in Green Tea and Model Systems. *Journal of Agricultural and Food Chemistry*, *67*(4), 1254-1260.

519 Kim, C. T., Hwang, E., & Lee, H. J. (2005). Reducing Acrylamide in Fried Snack Products by
520 Adding Amino Acids. *Journal of Food Science*, *70*(5), 354-358.
521 Koutsidis, G., Simons, S. P., Thong, Y. H., Haldoupis, Y., Mojica-Lazaro, J., Wedzicha, B. L., &
522 Mottram, D. S. (2009). Investigations on the effect of amino acids on acrylamide, pyrazines, and
523 Michael addition products in model systems. *Journal of Agricultural and Food Chemistry*, *57*(19),
524 9011-9015.
525 Martins, S. I., Jongen, W. M., & Van Boekel, M. A. (2000). A review of Maillard reaction in food
526 and implications to kinetic modelling. *Trends in Food Science and Technology*, *11*(9-10), 364-
527 373.
528 Mestdagh, F., Maertens, J., Cucu, T., Delporte, K., Van Peteghem, C., & De Meulenaer, B. (2008).
529 Impact of additives to lower the formation of acrylamide in a potato model system through pH
530 reduction and other mechanisms. *Food Chemistry, 107*(1), 26-31.
531 Nguyen, H. T., Van Der Fels-Klerx, H. J., & van Boekel, M. A. (2016). Kinetics of Nε-
532 (carboxymethyl) lysine formation in aqueous model systems of sugars and casein. *Food*
533 *Chemistry*, *192*, 125-133.
534 Nguyen, H. T., & Van Boekel, M. A. J. S. (2017). Acrylamide and 5-hydroxymethylfurfural
535 formation during biscuit baking. Part II: Effect of the ratio of reducing sugars and
536 asparagine. *Food Chemistry*, *230*, 14-23.
537 Poulsen, M. W., Hedegaard, R. V., Andersen, J. M., de Courten, B., Bügel, S., Nielsen, J., &
538 Dragsted, L. O. (2013). Advanced glycation endproducts in food and their effects on health. *Food*
539 *and Chemical Toxicology*, *60*, 10-37.
540 Qin, Y., Shin, J. A., & Lee, K. T. (2019). Determination of acetaldehyde, methanol and fusel oils in

distilled liquors and sakès by headspace gas chromatography. *Food Science and Biotechnology*, 1-7.

Scheijen, J. L., & Schalkwijk, C. G. (2014). Quantification of glyoxal, methylglyoxal and 3-deoxyglucosone in blood and plasma by ultra performance liquid chromatography tandem mass spectrometry: evaluation of blood specimen. *Clinical Chemistry and Laboratory Medicine*, *52*(1), 85-91.

Singh, R., Barden, A., Mori, T., & Beilin, L. (2001). Advanced glycation end-products: A review. *Diabetologia*, *44*, 129−146.

Srey, C., Hull, G. L., Connolly, L., Elliott, C. T., Del Castillo, M. D., & Ames, J. M. (2010). Effect of inhibitor compounds on N ε-(carboxymethyl) lysine (CML) and N ε-(carboxyethyl) lysine (CEL) formation in model foods. *Journal of Agricultural and Food Chemistry*, *58*(22), 12036-12041.

Stadler, R. H., Blank, I., Varga, N., Robert, F., Hau, J., Guy, P. A., Robert, M.C., & Riediker, S. (2002). Food chemistry: acrylamide from Maillard reaction products. *Nature*, *419*, 449−450.

Starowicz, M., & Zieliński, H. (2019). How Maillard reaction influences sensorial properties (color, flavor and texture) of food products?. *Food Reviews International*, *35*(8), 707-725.

Totsuka, Y., Ushiyama, H., Ishihara, J., Sinha, R., Goto, S., Sugimura, T., & Wakabayashi, K. (1999). Quantification of the co-mutagenic β-carbolines, norharmane and harmane, in cigarette smoke condensates and cooked foods. *Cancer letters*, *143*(2), 139-143.

Uchiyama, S., Inaba, Y., & Kunugita, N. (2011). Derivatization of carbonyl compounds with 2, 4-dinitrophenylhydrazine and their subsequent determination by high-performance liquid chromatography. *Journal of Chromatography B*, *879*(17-18), 1282-1289.

563 Van Boekel, M. A. J. S. (2006). Formation of flavour compounds in the Maillard
564 reaction. *Biotechnology Advance*, *24*(2), 230-233.
565 Wang, H. Y., Qian, H., & Yao, W. R. (2011). Melanoidins produced by the Maillard reaction:
566 Structure and biological activity. *Food Chemistry*, *128*(3), 573-584.
567 Yan, Y., Zeng, M. M., Zheng, Z. P., He, Z. Y., Tao, G. J., Zhang, S., Gao, Y., & Chen, J. (2014).
568 Simultaneous Analysis of PhIP, 4′-OH-PhIP, and Their Precursors Using UHPLC–
569 MS/MS. *Journal of Agricultural and Food Chemistry*, *62*(48), 11628-11636.
570 Yaylayan, V. A., Wnorowski, A., & Perez Locas, C. (2003). Why asparagine needs carbohydrates
571 to generate acrylamide. *Journal of Agricultural and Food Chemistry*, *51*(6), 1753−1757.
572 Yu, H., Zhong, Q., Xie, Y., Guo, Y., Cheng, Y., & Yao, W. (2020). Kinetic study on the generation
573 of furosine and pyrraline in a Maillard reaction model system of D-glucose and L-lysine. *Food*
574 *Chemistry*, 126458.
575 Yu, L., Chai, M., Zeng, M., He, Z., & Chen, J. (2018). Effect of lipid oxidation on the formation of
576 Nε-carboxymethyl-lysine and Nε-carboxyethyl-lysine in Chinese-style sausage during
577 storage. *Food Chemistry*, *269*, 466-472.
578 Zamani, E., Shokrzadeh, M., Fallah, M., & Shaki, F. (2017). A review of acrylamide toxicity and
579 its mechanism. *Pharmaceutical and Biomedical Research*, *3*(1), 1-7.
580 Zhang Y., Ren Y., & Zhang Y. (2009). New research developments on acrylamide: analytical
581 chemistry, formation mechanism, and mitigation recipes. *Chemical Review*, *109*(9): 4375-4397.
582 Zhang, Y., Ren, Y., Jiao, J., Li, D., & Zhang, Y. (2011). Ultra high-performance liquid
583 chromatography-tandem mass spectrometry for the simultaneous analysis of asparagine, sugars,
584 and acrylamide in Maillard reactions. *Analytical Chemistry*, *83*(9), 3297-3304.

585 Zhang, Y., Wang, Q., Huang, M., & Chen, X. (2015). Unravelling the effect of flavonoids on the
586 kinetic profiles of acrylamide in the Maillard reaction. *RSC Advance*, *5*(102), 84084-84092.
587 Zyzak, D. V., Sanders, R. A., Stojanovic, M., Tallmadge, D. H., Eberhart, B. L., Ewald, D. K.,
588 Gruber, D. C., Morsch, T. R., Strothers, M. A., Rizzi, G. P., & Villagran, M. D. (2003).
589 Acrylamide formation mechanism in heated foods. *Journal of Agricultural and Food*
590 *Chemistry, 51*(16), 4782-4787.
591

**Figure captions**

**Figure 1.** Kinetic profiles of glucose and amino acid (Lys, Trp, and Asn) in ~~the~~ different amino acid/glucose model systems when heated at 100 °C (A, C) and 130 °C (B, D). Asn/Glu: asparagine and glucose model system, Trp/Glu: tryptophan and glucose model system, Lys/Glu: lysine and glucose model system; Mix/Glu: asparagine, tryptophan, lysine and glucose model system.

**Figure 2.** Kinetic profiles of Maillard reaction harmful products ~~includes~~ including acrylamide (A), harmane (B), norharmane (C), CML (D), CEL (E), and melanoidins (F and G) in the different amino acid/glucose model systems when heated at 100 °C and 130 °C. Different alphabetical symbols shows significant differences ($p < 0.05$) in the content of acrylamide, CML, CEL, harmane and norharmane. Asn/Glu: asparagine and glucose model system, Trp/Glu: tryptophan and glucose model system, Lys/Glu: lysine and glucose model system; Mix/Glu: asparagine, tryptophan, lysine and glucose model system.

**Figure 3.** Kinetic profiles of α-dicarbonyl intermediate compounds, including glyoxal and methylglyoxal, in the different amino acid/glucose model systems when heated at 100 °C (A, C) and 130 °C (B, D). Asn/Glu: asparagine and glucose model system, Trp/Glu: tryptophan and glucose model system, Lys/Glu: lysine and glucose model system; Mix/Glu: asparagine, tryptophan, lysine and glucose model system.

**Figure 4.** Kinetic profiles of major aldehyde intermediate compounds, such as acrolein and acetaldehyde, in ~~the~~ different amino acid/glucose model systems when heated at 100 °C (A, C) and 130 °C (B, D). Asn/Glu: asparagine and glucose model system,

Trp/Glu: tryptophan and glucose model system, Lys/Glu: lysine and glucose model system; Mix/Glu: asparagine, tryptophan, lysine and glucose model system.

**Figure 5.** Postulated reaction scheme for simultaneous acrylamide, CML, CEL, harmane and norharmane formation ~~of~~ in asparagine, tryptophan, lysine and glucose Maillard reaction model system.

**Supplementary Figure 1.** Rate equations derived from the kinetic mechanism. [Glu] = glucose, [Lys] = lysine, [AAs] = amino acids, [Acr] = acrylamide, [Go] = glyoxal, [MGO] = methylglyoxal, [Trp] = tryptophan, [AP] = Amadori product, [Acro] = acrolein, [Ace] = acetaldehyde, [Asn] = asparagine, [CML] = $N^{\varepsilon}$-(~~Carboxymethyl~~carboxymethyl)lysine, [CEL] = $N^{\varepsilon}$-(~~Carboxyethyl~~carboxyethyl)lysine, [Har] = harmane, [Nor] = norharmane, [Mel] = melanoidins. $k_1$ ~~–~~ $k_{11}$ = rate constants (see Table 1).

**Supplementary Figure 2.** (A) Chromatograms for the determination of CML, CEL, GO and MGO; (B) Chromatograms for the determination of harmane, norharmane and glucose; (C) Chromatograms for the determination of lysine, asparagine and tryptophan; (D) Chromatograms for the determination of acrylamide acrolein and acetaldehyde.

**Table 1.** Estimation of kinetic parameters among different amino acid model systems.

| Group/T (°C) | Kinetics parameters[a] | | | | | | | | | |
|---|---|---|---|---|---|---|---|---|---|---|
| | $K_1$ ($10^{-3}$) | $R^2$ | $K_2$ ($10^{-2}$) | $R^2$ | $K_3$ ($10^3$) | $R^2$ | $K_4$ ($10^2$) | $R^2$ | $K_5$ ($10^2$) | $R^2$ |
| Lys-Glu/100 °C | 8.34 | 0.91 | 0.66 | 0.95 | 2.94 | 0.82 | 0.25 | 0.81 | - | |
| Trp-Glu/100 °C | 0.02 | 0.78 | 0.20 | 0.96 | - | | - | | - | |
| Asn-Glu/100 °C | 1.80 | 0.93 | 0.16 | 0.99 | - | | - | | - | |
| Mix-Glu/100 °C | 5.58 | 0.89 | 0.68 | 0.95 | 1.19 | 0.90 | 0.19 | 0.93 | - | |
| Lys-Glu/130 °C | 8.15 | 0.76 | 3.70 | 0.93 | 6.11 | 0.81 | 1.25 | 0.91 | - | |
| Trp-Glu/130 °C | 3.15 | 0.91 | 1.55 | 0.94 | - | | - | | - | |
| Asn-Glu/130 °C | 4.43 | 0.79 | 3.16 | 0.95 | - | | - | | 6.05 | 0.81 |
| Mix-Glu/130 °C | 4.67 | 0.83 | 4.05 | 0.89 | 1.91 | 0.83 | 0.77 | 0.93 | 1.09 | 0.89 |

a Data were expressed as mean ± SD in triplicates ($n$ = 3) and fit by the non-linear curve fitting method

633 **Table 1.** Continued

| Group/T (°C) | Kinetics parameters[a] | | | | | | | | | | | |
|---|---|---|---|---|---|---|---|---|---|---|---|---|
| | $K_1$ ($10^{-3}$) | $R^2$ | $K_2$ ($10^{-2}$) | $R^2$ | $K_3$ ($10^3$) | $R^2$ | $K_4$ ($10^2$) | $R^2$ | $K_5$ ($10^2$) | $R^2$ | $K_1$ ($10^{-3}$) | $R^2$ |
| Lys-Glu/100 °C | 0.27 | 0.88 | 1.50 | 0.77 | - | | - | | - | | 1.41 | 0.98 |
| Trp-Glu/100 °C | 0.16 | 0.77 | 0.94 | 0.79 | - | | - | | - | | 0.11 | 0.83 |
| Asn-Glu/100 °C | 0.15 | 0.81 | 0.63 | 0.75 | - | | - | | - | | 0.59 | 0.99 |
| Mix-Glu/100 °C | 0.19 | 0.80 | 0.79 | 0.79 | - | | - | | - | | 1.76 | 0.98 |
| Lys-Glu/130 °C | 1.58 | 0.98 | 11.4 | 0.79 | - | | - | | - | | 1.58 | 0.94 |
| Trp-Glu/130 °C | 1.09 | 0.96 | 9.58 | 0.80 | - | | 4.47 | 0.78 | 8.35 | 0.87 | 0.65 | 0.97 |
| Asn-Glu/130 °C | 5.77 | 0.98 | 445 | 0.77 | 4.41 | 0.92 | - | | - | | 1.21 | 0.95 |
| Mix-Glu/130 °C | 5.03 | 0.92 | 405 | 0.83 | 4.02 | 0.88 | 4.79 | 0.77 | 7.84 | 0.90 | 1.66 | 0.92 |

634
635

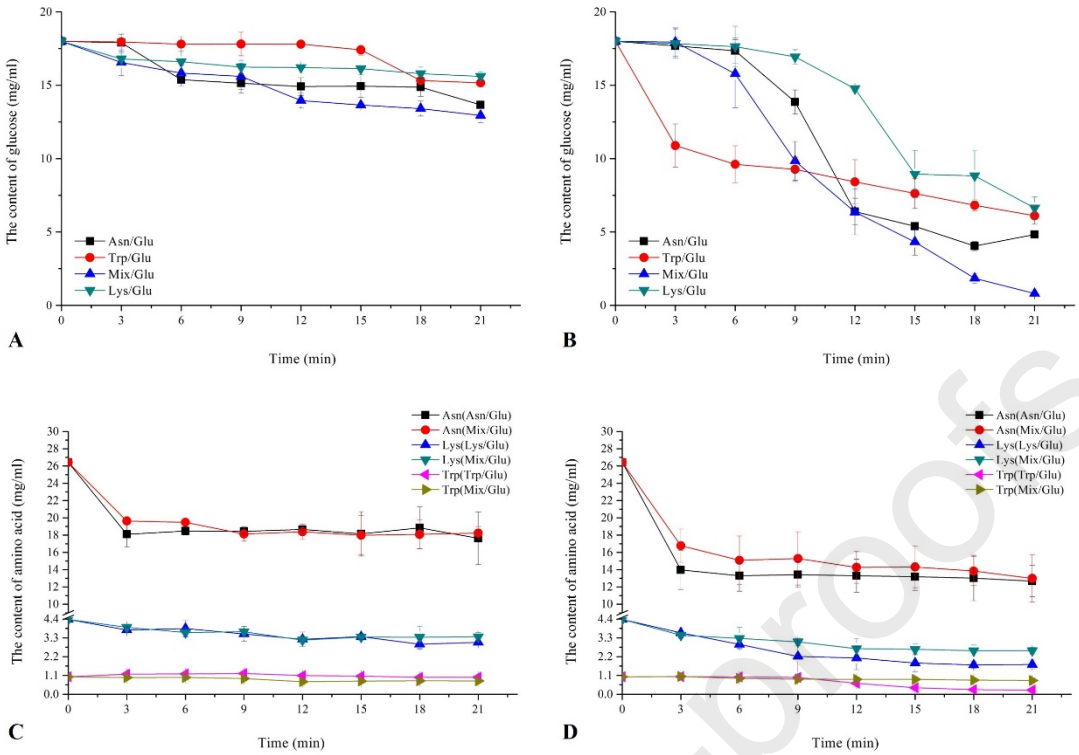


636

637 **Fig. 1**

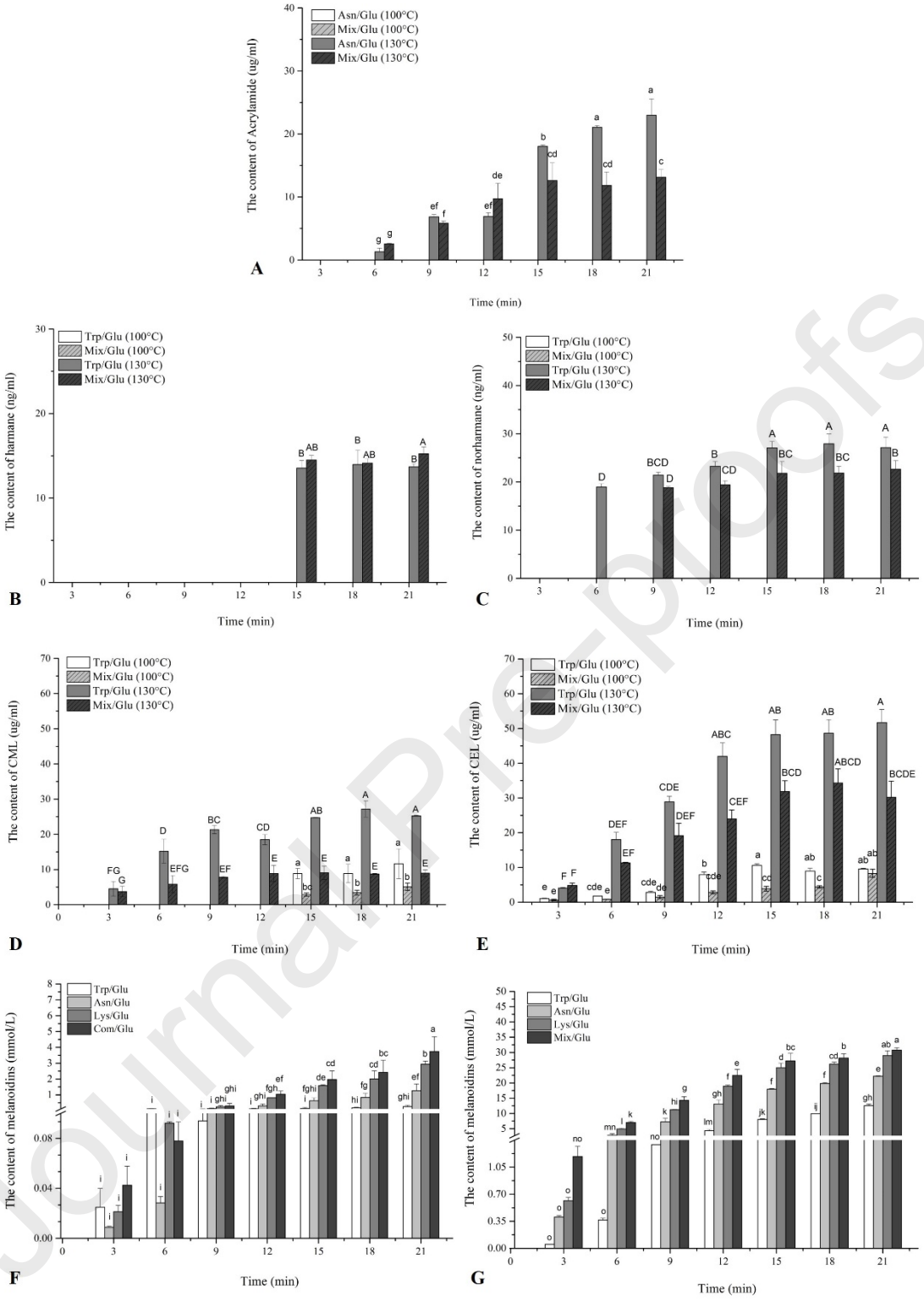


638

639 **Fig. 2**

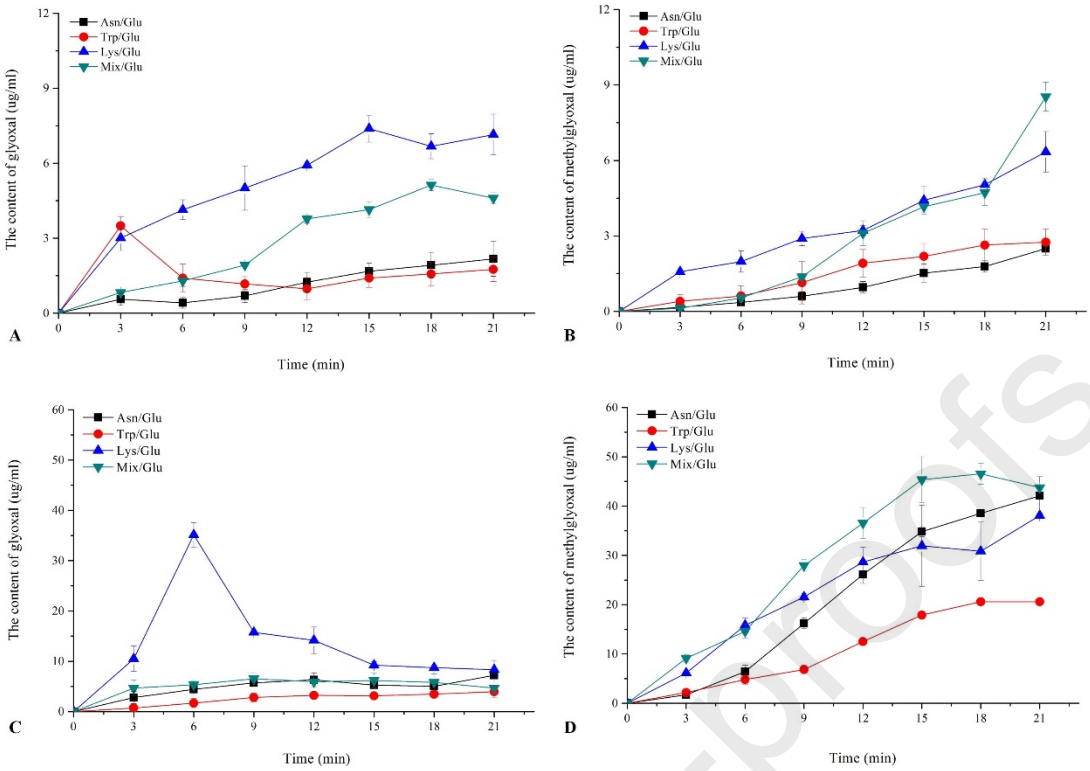


640

641 **Fig. 3**

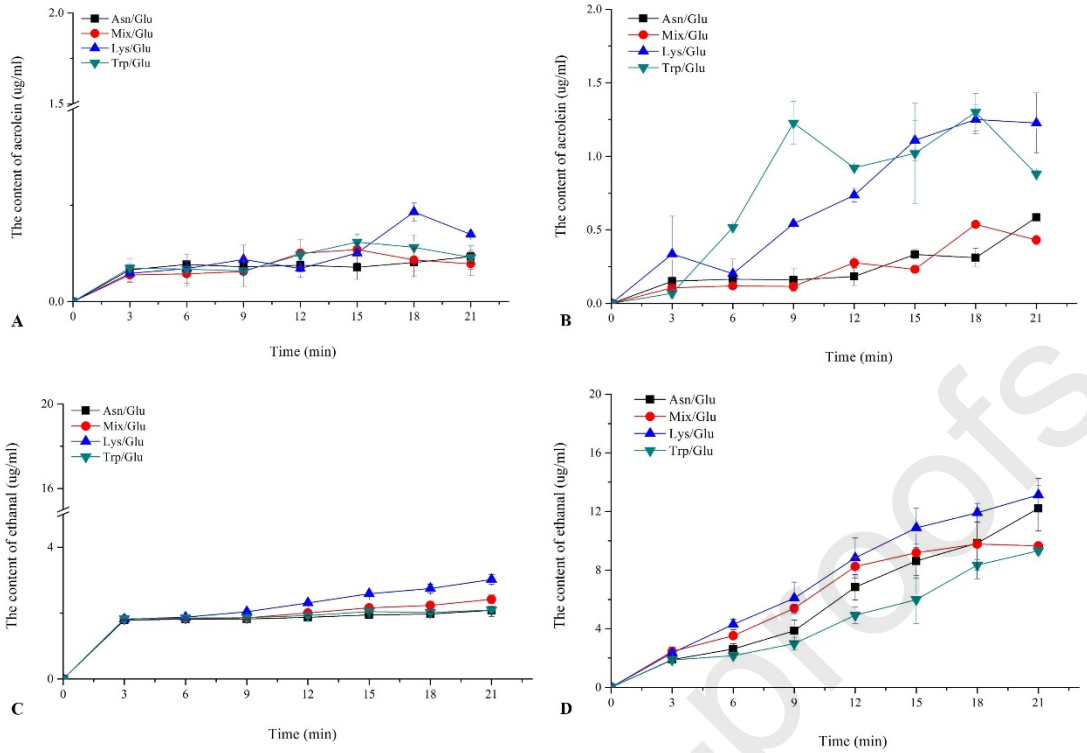


642

643 **Fig. 4**

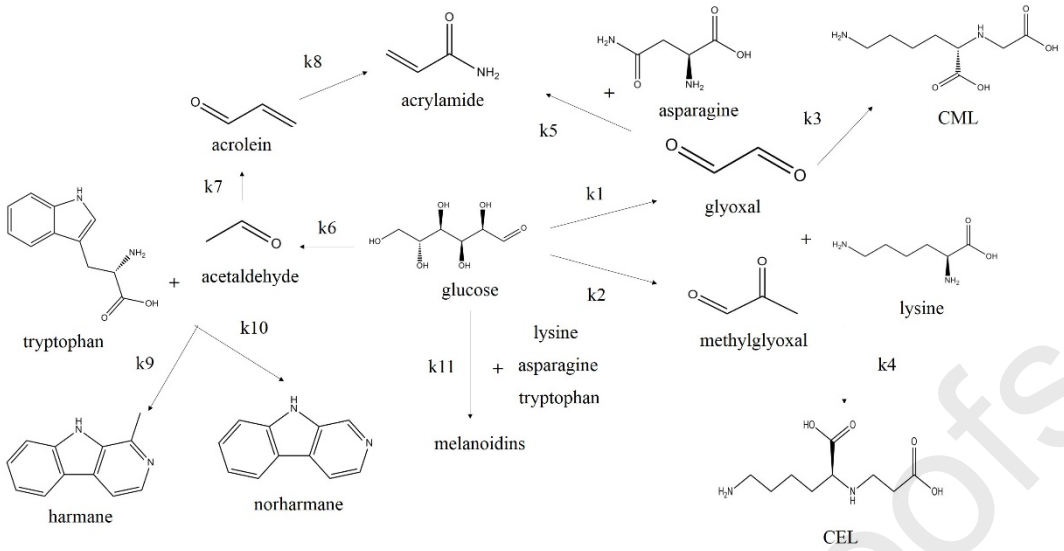


644

645 **Fig. 5**

Credit Author Statement

**Wei Quan:** Data curation, Writing- Original draft preparation, Investigation. **Yong Li**: Writing Review & Editing, Software. **Ye Jiao:** Formal analysis, Software. **Chaoyi Xue:** software. **Guoping Liu:** Vaildation. **Zhaojun Wang:** Resource. **Zhiyong He:** Methodology. **Guanjun Tao:** Software. **Fang Qin:** Supervison. **Jie Chen:** Project administration, Funding acquisition. **Maomao Zeng:** Writing Review & Editing, Funding acquisition.

**Declaration of interests**

☒ The authors declare that they have no known competing financial interests or personal relationships that could have appeared to influence the work reported in this paper.

☐The authors declare the following financial interests/personal relationships which may be considered as potential competing interests:

## Highlights

1. CML and CEL were formed in a model system heated to 100 °C
2. Asn and Trp competed with Lys for GO and MGO when heated to 100 °C
3. Harmane formed *via* Pictet-Spengler condensation between Trp and acetaldehyde

4. Asn competed with Lys for glucose, GO and MGO when heated at 130 °C
5. Trp inhibited the formation of acrylamide *via* the acrolein oxidation pathway